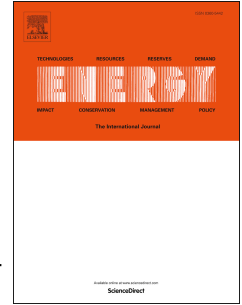


Accepted Manuscript

An optimal versatile control approach for plug-in electric vehicles to integrate renewable energy sources and smart grids

Omid Rahbari, Majid Vafaeipour, Noshin Omar, Marc A. Rosen, Omar Hegazy, Jean-Marc Timmermans, Mohammadreza Heibati, Peter Van Den Bossche



PII: S0360-5442(17)30998-2

DOI: [10.1016/j.energy.2017.06.007](https://doi.org/10.1016/j.energy.2017.06.007)

Reference: EGY 11011

To appear in: *Energy*

Received Date: 4 November 2016

Revised Date: 3 May 2017

Accepted Date: 1 June 2017

Please cite this article as: Rahbari O, Vafaeipour M, Omar N, Rosen MA, Hegazy O, Timmermans J-M, Heibati M, Bossche PVD, An optimal versatile control approach for plug-in electric vehicles to integrate renewable energy sources and smart grids, *Energy* (2017), doi: 10.1016/j.energy.2017.06.007.

This is a PDF file of an unedited manuscript that has been accepted for publication. As a service to our customers we are providing this early version of the manuscript. The manuscript will undergo copyediting, typesetting, and review of the resulting proof before it is published in its final form. Please note that during the production process errors may be discovered which could affect the content, and all legal disclaimers that apply to the journal pertain.

1 An optimal versatile control approach for plug-in electric 2 vehicles to integrate renewable energy sources and smart grids

3 Omid Rahbari^{a*}, Majid Vafaeipour^a, Noshin Omar^a, Marc A. Rosen^b, Omar Hegazy^a, Jean-Marc Timmermans^a,
4 Mohammadreza Heibati^c, Peter Van Den Bossche^a

5 ^a Vrije Universiteit Brussel (VUB), Pleinlaan 2, MOBI Research Group and ETEC Dept., Brussel 1050, Belgium

6 ^b Faculty of Engineering and Applied Science, University of Ontario Institute of Technology, Oshawa, Ontario, L1H
7 7K4, Canada

8 ^c Department of Civil Engineering, University of Ottawa, 161 Louis Pasteur, A705 Ontario K1N6N5, Canada

9 **Highlights:**

- 10 • Optimization problems are solved to size and site smart parking lots of electric vehicles.
- 11 • The effectiveness of the proposed algorithm is compared to other reported algorithms.
- 12 • An adaptive intelligent control strategy with V2G and G2V applicability is proposed.
- 13 • A global optimal solution is guaranteed with the proposed model.

14 **Abstract**

15 This study proposes a practical solution to deal with challenges of integrating renewable
16 energy sources and electric vehicles into the electric grid, considering generation source
17 intermittency and energy usage inconsistency, via a new adaptive intelligent controller. The
18 present research describes a smart grid consisting of power plants and distributed generation,
19 fueled via photovoltaic panels and wind turbines, and augmented with electric vehicles as power
20 storage devices. Employing a parking lot to deal with challenges such as low penetration of the
21 electric vehicles embedded with Vehicle-to-Grid functionalities encounters two difficulties:
22 where they should be installed, and modeling of bi-directional power flow between electric
23 vehicles, the grid, and the distributed generation system. In this regard, a nonlinear multi-
24 objective problem is designed and solved via employing the Non-dominated Sorting Genetic
25 Algorithm-II, and the forward and backward substitution method. In addition, Newton-Raphson
26 Power Flow is adopted and modified to calculate the power flow of the distribution network. The
27 results related to optimal placement and sizing of hybrid renewable energy systems show that
28 bus 16 of the studied grid is the best place to integrate a parking lot – equipped with 117
29 photovoltaic and 10 wind turbine units - to the tested IEEE-26 buses. Furthermore, this study
30 suggests that the aforementioned grid could employ a complex versatile control unit able to

* Corresponding author:

Email address: Rahbari.omid@gmail.com

Cell Phone: (+32)485-160-630

31 optimize the operating point, scheduling charging and discharging for a large number of electric
 32 vehicles while considering the technical aspects (total active power loss and voltage deviation).
 33 In this regard, a new hybrid control approach based on Particle Swarm Optimization-Adaptive
 34 Neuro-Fuzzy Inference System tuned via utilizing the optimal power flow problem is proposed.
 35 The controller's superiority to handle grid-to-vehicle and vehicle-to-grid services is discussed
 36 and compared to other studies.

37 **Keywords:** *Smart Grid; Electric Vehicle; Renewable energy sources; Distributed Generation;*
 38 *PSO-ANFIS controller;*

39 Acronyms

ANN	Artificial neural network	O&M	Operation and maintenance
ANFIS	Adaptive Neuro-Fuzzy Inference	PHEV	Plug-in Hybrid Electric Vehicle
ADN	Active distributed network	PSO	Particle Swarm Optimization
BEV	Battery Electric Vehicle	PS	Power system
DG	Distributed Generation	PV	Photovoltaic
DR	Demand response	PQ	Real and reactive power injections are fixed
ESS	Energy storage system	PV_b	Real power and voltage magnitude are fixed
EV	Electric vehicle	RG	Renewable generation
G2V	Grid-to-vehicle	RES	Renewable energy system
GV	Grid vehicle	SVD	Summation of voltage deviation
GHG	Greenhouse gas	SG	Smart Grid
HRES	Hybrid Renewable Energy System	SoC	State of charge
NN	Neural network	V2G	Vehicle-to-grid
OPF	Optimal power flow	WT	Wind turbine
OF	Objective function		

40

41 Nomenclature

42

P_{Loss}	Active power loss	$P_{DG,i}^{\min}$	Minimum power out of DG
$P_{DG-i,k}$	Active power of i th DG unit at k th time period	$P_{DG,i}^{\max}$	Maximum power out of DG
C_1, C_2	Acceleration factor	R_{ij}, Z_{ij}	Resistance of line

τ	Average capacity coefficient	$C_{O\&M-i}$	Maintenance cost of i th DG unit
$P_{disch,t}$	Discharge power	n	Operational life of i th DG unit
$P_{ch,t}$	Charge power	$\delta_{ij}, \delta_i, \delta_j$	Phase angles
$g_i(u, x)$	Equality constraints	Q_0	Population of offspring
r	Fixed annual interest rate	$V_i^{k,spec}$	Specified voltage magnitude
$h_i(u, x)$	Inequality constraints	f_1	Summation of voltage deviation objective
P_{I-i}	installation cost of i th DG unit	X	State variables
C_{I-i}	investment cost of i th DG	N_h	Total simulation hours
ij	Index of buses	f_2	Total active power loss objective
k	Index of time	f_3	Total annual investment and operation cost objective
$P_{Grid,t}$	Grid power at time t	$P_{PV,t}$	Total PV power
t_k	k th time segment	$P_{Wind,t}$	Total wind power
m	Number of DG units of a type	N_{DG}	Total number of DG units
N	Number of buses	V_i^k	Voltage magnitude
N_{DG}	Number of DG units	u, v	Vectors of control variables
$V_i^{k,max}$	Maximum voltage limitation	$x_{1,t}, x_{N_{vehicles},t}$	Decision variables
$V_i^{k,min}$	Minimum voltage limitation		

43 1. Introduction

44 Recent studies indicate that the world's energy demand will increase by 56% from 2010 to
45 2040 [1], with an expected increase in carbon dioxide annual emissions from 31.2 to 45.5 billion
46 metric tons. Meanwhile, the energy market is confronted with greater challenges such as
47 diminishing reserves of fossil fuels, lack of energy security, and economic and urbanization
48 growth [2]. The existing circumstances and the future gap between energy demand and supply,
49 as well as greenhouse gas emissions, compel scientists to follow two strategies, among others:
50 substitution of using renewable energy sources for fossil-based power generating units, and
51 improving energy efficiency [3]. The electrical power generation industry and the transportation

52 sector – which were responsible for almost 27% of total energy consumption [4] and 33.7% of
53 greenhouse gas (GHG) emissions in 2012 – are still excessively reliant on fossil fuels [5]. These
54 concerns and the proliferation of electric vehicles (EVs) in recent years have led engineers to
55 provide solution to challenges with EVs and create opportunities to the power industry. The
56 former is undergoing a transformation from traditional power systems (PSs) to Smart Grids
57 (SGs). Regarding increasing energy efficiency, efforts are concerned with the overall process of
58 electricity production and use, from power plants to final users. Note that location and
59 availability of energy resources, as well as having low cost and/or being renewable, play a
60 prominent role in augmentation of energy efficiency. When concern is focused on electricity
61 processes, aspects of efficiency to be accounted for include those related to generation,
62 utilization and transmission; efforts include the introduction of highly efficient generators,
63 motors, and drives to reduce losses [6].

64 A significant proportion of losses in electrical power systems (distribution, transmission and
65 generation) is associated with the distribution system, where approximately 13% of the total
66 power produced is lost [7]. Consequently, power loss reduction in the distribution section has
67 been an important goal for researchers and engineers. A high proportion of the losses in the
68 distribution section can be mitigated through the use of distributed generation (DG) units, which
69 typically are small generators. Furthermore, EVs not only act as a load in the system of grid-to-
70 vehicle (G2V), but also as a storage in the system of vehicle-to-grid (V2G); vehicles are parked
71 roughly 95% of the time [8], allowing them to be used to feed PSs using their batteries. EVs and
72 renewable energy systems (RESs) are categorized as distributed power storage and generation
73 units to support the grid [9]. However, EVs and RESs face a number of difficulties; when the
74 former are fed with the latter with poor regulation, the distribution infrastructure may be
75 undermined and subject to severe stresses. This adversely affects power quality on a local scale
76 and degrades system efficiency, especially when combined with the fact that power generation
77 from RESs is directly linked to climatic and weather conditions. In this regard, integration of
78 electric vehicles and RESs in power systems is an effective method to achieve peak shaving,
79 voltage regulation, frequency regulation, load leveling, and other ancillary services [10]. But
80 successful integration of RESs and EVs with PSs is unlikely without a more controllable system
81 having good coordination of EVs (G2V, V2G), RESs and PSs relying on bi-directional smart

82 grid communication infrastructure, which has the ability to handle the information that must be
83 exchanged among different entities.

84 **1.1. Literature review**

85 In power systems, an effective mechanism for achieving energy efficiency is demand response
86 (DR), in which demand for electricity is managed in response to severe times (e.g., when load
87 exceeds generation, often during peak demand periods) or to market price in a smart grid
88 environment. Progressive communication infrastructure provides two ways (power line
89 communications and wireless sensor networks) for information on energy supply and demand to
90 be used to enhance the DR capabilities of entire power systems. Indeed, employing
91 communication techniques is the main purpose of introducing more intelligence in control for
92 distributing electric energy from supplies to consumers. As addressed in [11], the backbone of a
93 smart grid accentuates environmental protection, by using variable generation types (such as
94 wind and solar), demand response, and distributed generation encompassing EV technology, in
95 order to achieve better asset utilization while maintaining reliable system operation and
96 recognizing the need for enhanced customer choice. Fig. 1 depicts these factors in relation to the
97 new emerging smart grid paradigm, and illustrates the role of EV technology in the new era.



98
99 Figure 1. EVs in relation to the new emerging smart grids [11]

100 To explore the main technological challenges and to identify beneficial opportunities, Yu et
101 al. [12] explored the main concepts of smart grids and concluded that advantages from those
102 systems can be only attained in presence of integrated systems rather than standalone ones. The
103 optimal integration of energy storage systems into the grid can offers opportunities for demand

104 side management, load shifting, peak shaving and reducing power losses. Shaaban et al. [13]
105 performed a multi-objective optimal siting and sizing of renewable energy systems for a 33-bus
106 grid by identifying optimal buses for installing renewable distributed generation; this was done
107 to maximize the savings through allowing system upgrade investment deferrals, and reducing
108 costs of annual energy losses and interruptions. Feruzzi et al. [14] examined a demand side
109 management optimization technique and performed a sensitivity analysis for a micro-grid
110 including a photovoltaic plant. They demonstrated the effectiveness of shifting the load from
111 high energy price hours to low energy price hours and its economic benefits. EVs can not only
112 contribute as energy storage systems for smart grids using vehicles integrated to grid
113 infrastructures in support of appropriate demand response programs, but also can be used to
114 overcome the vagaries of generation caused by inherent uncertainties of renewable energy. In
115 this regard, Vasirani et al. [15] evaluated an agent-based approach to take the advantage of using
116 EVs as storage systems to increase the profit and reliability of intermittent wind energy and also
117 scheduling the supply to grid and storage in EVs via linear-programming. Integration of EVs into
118 the grid requires appropriate management and control of EVs charging/discharging times,
119 considering driving needs and simultaneous support of power services simultaneously [16]. By
120 including vehicle-to-grid capability as an energy storage management technique, López et al.
121 [17] utilized an optimization-based model in a smart grid environment for load shifting purposes.
122 The study was performed on a 27-bus IEEE distribution grid considering load curve, mobility
123 requirements of EVs, and hourly process configurations to allocate the demand more efficiently.
124 Moreover, they reported that large fleets of EVs should be considered for attaining significant
125 improvements in peak shaving and load flattening.

126 Sovacool and Hirsh [18] investigated the socio-technical barriers of transitioning to PHEVs
127 and V2G systems, and focused on the technological, cultural, social, and political challenges.
128 These need to be addressed to benefit from the services and revenues of such systems. Sovacool
129 and Hirsh identified control strategies and battery improvements for widespread utilization of
130 PHEVs and V2G technologies. Graditi et al. [19] investigated the economic viability of utilizing
131 battery energy storage systems for load shifting at a consumer level for specific electricity tariffs,
132 and suggested such systems as future competitive technologies. Graditi et al. stated that techno-
133 economic analyses of such systems when integrated with renewable energy systems are merited.
134 In an overview of battery management systems and their significance, Rahimi-Eichi [20]

135 evaluated opportunities, needs and challenges of integrating renewable energy, smart grids and
136 EVs via focusing on power delivery, lifetime, cost, reliability and SoC. They noted that SoC
137 estimation techniques are an essential aspect, which needs research and development for
138 satisfying the standards for smart grid and EV applications. In an optimization study, Silvestre et
139 al. [21] considered the initial SoC and load consumption profile of EVs to minimize the power
140 losses and energy costs via smart charging. It was noted that a majority of PEVs utilize lithium
141 ion (Li-ion) batteries because of the environmental advantages, light weight, longer life span, and
142 higher energy density [22]. Omar et al. [23] demonstrated that the energy efficiency of lithium-
143 ion batteries is far superior to other rechargeable energy storage types, based on tests of dynamic
144 discharging performance. Moreover, they showed that the performance of Li-ion batteries is
145 highly dependent on temperature and depth of discharge [24]. In addition, it was indicated that
146 the life cycle is reduced for higher charge current rate cases, and suggested that Li-ion batteries
147 should not be subject to high charging rates.

148 Identifying the proper technical features and predicting realistic system behavior are required
149 to control large scale deployment of V2G systems. Arrival and departure times, charging period
150 and charging rates are significant aspects that should be managed and controlled for successful
151 coordination of PHEVs, PS and HRESs in smart grids. To evaluate the potential challenges of
152 smart grids, Waraich et al. [25] used an EV demand model combined with a power system
153 simulation to examine the potential challenges and capacity of the network for particular
154 penetration of EVs. Waraich et al. considered charging schemes and charging periods of the
155 vehicles in various scenarios. Haidar et al. [26] reviewed technical challenges of grid-integrated
156 electric vehicles and demonstrated that vehicle penetration, charging time, charging
157 characteristics, driving patterns and transportation network are significant system-dependent
158 factors for future practical utilization of grid-integrated electric vehicle systems. Little research
159 has been reported on control aspects of EVs, PSs and RESs. To introduce a smart EV charging
160 method for smart residences and buildings, an EV charging algorithm is proposed to determine
161 the optimal schedules of EV charging based on anticipated RES output and electric consumption
162 [27]. The results demonstrate the effectiveness of the proposed smart EV charging model.
163 Similarly, intelligent workplace parking is proposed for EVs in [28] involving a smart power
164 charging controller. Based on power requirements, a fuzzy logic power flow controller is
165 designed in which charging rates are dependent on the predicted power generation of the PV

166 output. The impacts of EV charging processes on the grid are compared with and without the
167 developed smart charging technique. Researchers have analyzed the application of V2G systems
168 as a power system regulator by utilizing aggregated EVs as a battery storage model in load
169 frequency control simulations [29]. The model is applied for power system regulation for typical
170 days with high and low wind energy in Denmark. The influence of EVs on PSs and their
171 capabilities have been examined by using load flow technique [30]. However, previous work has
172 not used smart control techniques to investigate charging or discharging of EVs energy in
173 interaction with the grid. ANN and ANFIS controllers have been employed for examining the
174 performance of those methods [31]. The results show that the controllers exhibit similar settling
175 times but there is difference in the power allowed by the controller to the flow between the PSs
176 and EVs. Moreover, as addressed in [32], two controllers based on fuzzy systems have been
177 designed, one controlling the G2V concept of EVs and the other designed based on the V2G
178 concept. In addition, controllers were tuned via knowledge and intuition of experts and the
179 parameters associated with membership functions.

180 **1.2. Motivation, objectives, and innovative contribution**

181 The main attributes of an optimum on-grid renewable-powered parking lot can be categorized
182 as follows:

- 183 • It is placed in an appropriate site in order to minimize the total active power loss as a
184 distributed generation resource, and the summation of voltage deviation. It is grid-
185 friendly and enhances power quality.
- 186 • It is a decentralized resource, and is integrated into an optimized renewable energy
187 system. It is cost-effective and considers sustainable development.

188 Furthermore, the key attributes of PSO-ANFIS controller can be categorized as follows:

- 189 • It controls power flow and optimizes the system stability in PSs.
- 190 • It has a significant impact on the performance of unified power flow between
191 components.

192 A precise estimation of the SoC is needed to determine the energy content of the battery and to
193 prevent damage associated with excessive depth of discharge. In this study, the inputs of the
194 proposed controller are designed using direct and indirect information regarding both grid and
195 battery characteristics. Voltage deviations are defined as indirect signals and charging rates are
196 defined as indirect signals. Also, SoC, which represents the percentage of the remaining capacity

197 or energy of the battery, is introduced as a direct signal for all individual vehicles, to prevent
 198 batteries from excessive discharge. Throughout the analysis, battery chargers are assumed to be
 199 off-board.

200 Via considering the literature and looking into functionalities of conventional EV charging
 201 controllers, Table 1 presents that the previously used controllers have limited functionality, do
 202 not provide a simultaneous smart control to: a) meet user's needs in terms of satisfactory
 203 charging time and energy content, b) support active network operation, and c) prolong EV
 204 battery life compared to the objectives of the present study. Along this line and to cover the
 205 previously mentioned gaps, the present article proposes a new adaptive controller which not only
 206 is capable of overcoming the challenges of voltage profile regulation, but also considers
 207 reduction of charging cycle, discharging cycle and power loss.

208 Table 1. The capability of proposed control in comparison with other studies

Controller	Objectives		
	Network support	User's requirements	Battery life extension
Standard EV charger	-	✓	-
Centralized aggregator [32, 33]	Partially (not in real-time)	✓	-
Decentralized controller [34]	✓	-	-
Centralized control [35]	-	✓	-
Proposed centralized control	(Totally real-time)	✓	✓

209

210 This paper, by proposing two strategies, extends our previous work [4] to address the
 211 aforementioned problems. The first strategy is associated with an optimal power flow, which
 212 provides useful information on the tradeoff between energy demand such as load demand and
 213 G2V processes, and energy generation such as grid, DG, and V2G processes. The second
 214 strategy is to build a highly-sensitive controller by observing the voltage profile and power loss
 215 fluctuation. The main objectives of this paper are as follows:

- 216 • To determine appropriate locations of smart parking lots and sizing of hybrid renewable energy
 217 systems (HRESs) through reducing total active power losses and enhancing grid characteristics
 218 such as voltage profile, via an evolutionary algorithm.

- 219 • To introduce a new intelligent operation, based on a hybrid PSO-ANFIS, by optimizing the
220 process of grid to vehicles, vehicles to grid consisting of hybrid renewable energy systems, and
221 power systems.

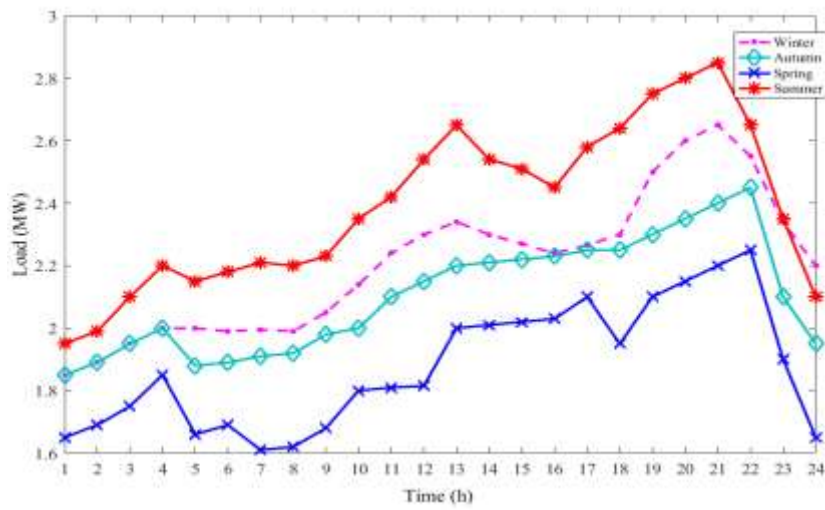
222 **2. Optimal siting and sizing of DG; formulation, constraints and algorithm**

223 As mentioned earlier, the present study desires to perform a multi-objective optimal sizing
224 and siting of smart parking lots in a power distribution network in order to develop an active
225 distributed network (ADN). In this regard, different criteria are considered in the optimization
226 process including voltage deviation, total active power loss and annual operation and
227 maintenance (O&M) costs of DG. The first and second optimization objectives are to decrease
228 the system voltage deviation and power losses. The third objective is to minimize the annual
229 O&M cost of DG. These three objectives involve different perspectives based on DG power
230 utilities and owners. For instance, adding more DGs to the distribution system can decrease
231 power losses, but it increases the voltage variation and O&M cost.

232 **2.1. Time sequence characteristic of load and DG**

233 To consider the required regulation in different seasons of the year, time-dependent load
234 curves on an hourly basis are considered for each season (see Fig. 2) in the present study.

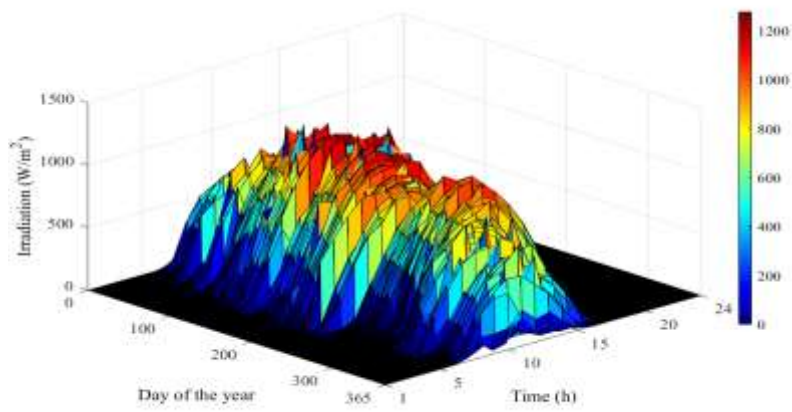
235 Due to the fact that the output of photovoltaic (PV) or wind turbine (WT) electrical generators
236 are significantly affected by geographical location and available natural wind and solar energy
237 sources, the assumption of constant DG outputs in all seasons is far from being realistic. Hence,
238 the average DG output capacity of 24 time periods in one day of each season is employed, and
239 different types of DG considering PV and WT power generation are considered in this paper.
240 Fig. 3 and Fig. 4 present one-year solar irradiation and wind velocity data for Tehran, Iran,
241 obtained from Iran National Meteorological Organization. These data are utilized for the purpose
242 of the present study.



243

244

Figure 2. Time sequence characteristic curves of seasonal load types



245

246

Figure 3. Hourly breakdown of annual solar radiation received on horizontal surface in Tehran, Iran

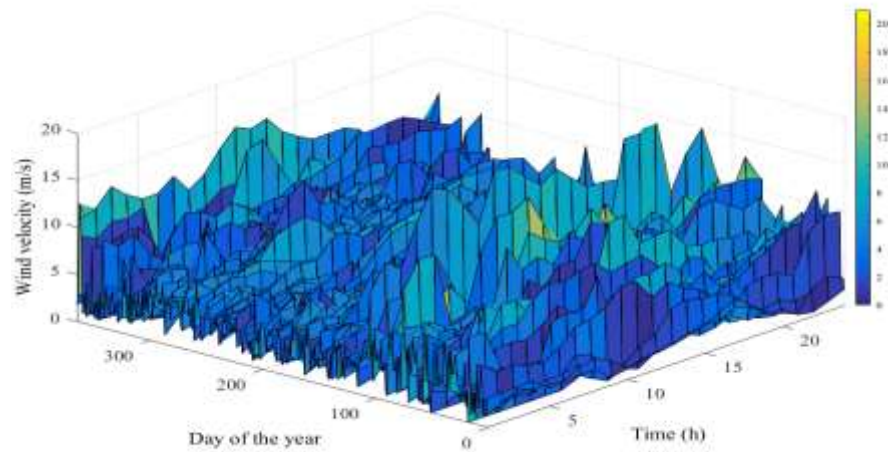


Figure 4. Hourly breakdown of annual wind velocity data for Tehran, Iran

2.2. Minimization of voltage deviation

The first objective is to minimize the voltage deviation between the nodal voltage and the specified voltage magnitude. The nodal voltage magnitude is a significant indicator for assessing power quality and system security. Lowering the voltage deviation can help provide a superior voltage level in the distribution system. This objective can be expressed as follows:

$$\min f_1(x) = \min \sum_{k=1}^{N_h} \left[\sum_{i=0}^N \left(\frac{V_i^k - V_i^{k,spec}}{V_i^{k,max} - V_i^{k,min}} \right)^2 \right] \quad (1)$$

where N_h , N , V_i^k and $V_i^{k,spec}$ are the total hours, the number of buses, the voltage magnitude at the i th bus of the k th time period and the specified voltage magnitude, respectively, while $V_i^{k,max}$ and $V_i^{k,min}$ are the upper and lower limits at the i th bus, respectively. The total hours N_h is equal to 24 h.

2.3. Minimize power losses

Power losses depend on two factors: current and line resistance. Line resistance is negligibly low [36]. Thus, the line loss is linked to the current, and the current line is related to the system topology and the loads. Note that decreasing the value of load demand, which is a function of time, is not feasible. Nevertheless, line currents can be reduced with proper placement of DGs. The total active power loss can be expressed as follows:

$$\min f_2(x) = \min \sum_{i=1}^N \sum_{\substack{j=1 \\ i \neq j}}^N R_{ij} \left(\frac{|V_i|^2 + |V_j|^2 - 2|V_i||V_j|\cos \delta_{ij}}{|Z_{ij}|^2} \right) \quad (2)$$

264 Here, P_{Loss} , R_{ij} , Z_{ij} , $|V_i|$ and δ_{ij} are the total network active power loss, the resistance of the line
 265 between the nodes i and j , the voltage magnitude and difference between δ_i and δ_j which are the
 266 angles at bus i and j , respectively.

267 2.4. Minimize annual investment and operation cost

268 For HRESs, there are no significant pollutant emissions in power generation due to the use of
 269 renewable energy. In order to consider the time sequence characteristic of DG, working
 270 scenarios at various time periods are calculated. Assuming the DG power output in each time
 271 segment remains constant, the annual O&M cost can be determined as follows [36]:

$$\min f_3(x) = \min \sum_{i=1}^{N_{DG}} \left((C_{I-i} + C_{O\&M-i}) \sum_{k=1}^{N_h} P_{DG-i,k} t_k \right) \quad (3)$$

272 where N_{DG} , C_{I-i} , $C_{O\&M-i}$, $P_{DG-i,k}$ and t_k are the number of DG units, the investment cost, the
 273 maintenance cost of the i th DG unit, the active power of the i th DG unit at the k th time period
 274 and the duration of the k th time segment, which is set to 1 hour in this study. Again, N_h is equal
 275 to 24 hours.

276 The investment cost C_{I-i} is calculated as follows:

$$C_{I-i} = \frac{r(1+r)}{(1+n)-1} \times \frac{P_{I-i}}{N_h \times \tau} \quad (4)$$

277 where n , τ and r are the operational life of the i th DG unit, the average capacity coefficient,
 278 which is equals to the annual power production by the rated power in one year, and the fixed
 279 annual interest rate, respectively. Also, P_{I-i} is the installation cost of i th DG unit.

280 2.5. Constraints

281 In the optimization model, three constraints are considered relating to power flow, DG
 282 capacity, and nodal voltage.

283 (1) Power flow equation: when “Smart Parking” for electric vehicles is treated as a load, the
 284 backward and forward substitution method is adopted to calculate the power flow of the
 285 distribution network. But when they are treated as a power supply, the Newton-Raphson power
 286 flow calculation is employed, which is appropriate for power flow calculations in a multi-power-
 287 source network [37]. That is,

$$P_{PV,t} + P_{Wind,t} + P_{Grid,t} + P_{disch,t} - P_{ch,t} - \sum_{i=1}^N \sum_{\substack{j=1 \\ i \neq j}}^N R_{ij} \left(\frac{|V_{i,t}|^2 + |V_{j,t}|^2 - 2|V_{i,t}||V_{j,t}|\cos \delta_{ij,t}}{|Z_{ij}|^2} \right) - P_{Load,t} = 0 \quad (5)$$

288 where $P_{PV,t}$, $P_{Wind,t}$ and $P_{Grid,t}$ are the powers obtained from PVs, wind units and the main grid,
 289 respectively, at time t , while $P_{disch,t}$ and $P_{ch,t}$ are the EV batteries charge power and discharge
 290 power, respectively, at time t . Note that $P_{disch,t}$ and $P_{ch,t}$ are calculated based on the initial SoC,
 291 presented in Appendix A, and using data on the arrival and departure times of the electric
 292 vehicles.

293 (2) Generation limits: The following generation limits apply:

$$P_{DGi}^{\min} \leq P_{DGi} \leq P_{DGi}^{\max} \quad (6)$$

294 (3) Load bus voltage constraints: The load bus voltage is constrained as follows:

$$V_i^{\min} \leq V_i \leq V_i^{\max} \quad (7)$$

295 In the above two inequality constraints, $P_{DG,i}^{\min}$ and $P_{DG,i}^{\max}$ denote the minimum and the
 296 maximum power generation levels from DG i , V_i^{\min} and V_i^{\max} are the minimum and maximum
 297 voltages of bus i .

298 2.6. Overview of optimal sizing and siting formulation

299 The present model is developed considering minimal setup and maintenance costs for the PVs
 300 and wind turbines, and minimal total active power losses and voltage deviations. Integrating the
 301 objectives and constraints, the problem can be considered as a nonlinear multi-objective
 302 problem, and formulated as follows:

303

$$\begin{aligned} \text{Minimize:} & \quad f(x,u) = (f_1(x,u), \dots, f_3(x,u)) \\ \text{Subject to:} & \quad g_i(u,x) = 0 \quad i = 1, \dots, n_{eq} \end{aligned} \quad (8)$$

$$h_i(u, x) \leq 0 \quad i = 1, \dots, n_{ineq}$$

304 Here n_{eq} and n_{ineq} denote the number of equality constraints and inequality constraints,
 305 respectively, u is the vector, which contains the control variables, and x is the vector of the state
 306 variables. The assumption in this section is that DG can be considered as a PQ bus and includes a
 307 constant power factor. The controlling variables consist of type, sizing, and placement of DG
 308 units.

309 To have a realistic situation for DG integration, the unit capacity of the PV and WT units are
 310 15 kW and 250 kW, respectively. Therefore, the total solar power and wind power generation
 311 coordinated with distribution network (DN) is $m_{PV} \times 15$ kW or $m_{WT} \times 250$ kW depending on the
 312 type of DG, where m denotes the number of DG units of a type. Integer coding is applied for the
 313 encoding the scheme, which is depicted as follows:

$$u = [Char_{DG_1}, PLC_{DG_1}, m_{DG_1}, \dots, Char_{DG_{N-DG}}, PLC_{DG_{N-DG}}, m_{DG_{N-DG}}] \quad (9)$$

314 Here, $Char_{DG}$, PLC_{DG} , m_{DG} , and $M-DG$ respectively denote the type, the location, the number
 315 of units of each DG unit and the maximum number of DG units, which are integrated into the
 316 distribution system.

317 2.7. NSGA-II algorithm

318 The NSGA-II, which evolved from Non-dominated Sorting Genetic Algorithm-II NSGA [38],
 319 is one of the first evolutionary algorithms and is used for optimal sizing and siting of the HRES
 320 in the present study. NSGA-II performs well and has proven useful for application in energy
 321 contexts. Recent applications in terms of electrical energy include the reconfiguration of a smart
 322 grid [39], the sizing of DG in a distribution system [36] and the optimization of the control of a
 323 doubly-fed induction generator for systems of wind energy [40]. The algorithm applies a fast
 324 non-dominating sorting procedure to find the optimal solution based on Pareto dominance [41].
 325 The Pareto-optimal decision vectors create a Pareto-optimal front in the search region (or
 326 feasible area). Like other population-based algorithms, NSGA-II is initiated with the random
 327 generation of parent individuals, P_0 , of latent solutions. The size of the parent population is N
 328 and it is controlled for domination of the Pareto and fitness values matching with a non-
 329 domination step allocated to every solution. Then, the algorithm applies the fitness value for
 330 ranking and assigning solutions to the varied fronts (i.e., each solution is related to varied fronts
 331 according to the domination level). The first front includes the solutions dominating the others.

332 The population of offspring, which is called Q_0 and whose size is as large as the parent's
 333 population, is produced according to tournament selection and mutation.

334 After producing the first generation, the method proceeds to combining the present population
 335 with the determined non-dominated solution. The entire method for the j^{th} generation is as
 336 follows:

- 337 1. parents and offspring populations are combined to produce R_j of size $2N$;
- 338 2. non-dominated sorting for R_j is applied to determine the varied fronts F_i ;
- 339 3. solutions of (F_1, \dots, F_n) are chosen to produce P_{j+1} of size N ;
- 340 4. tournament selection is applied according to crossover, crowding-comparison, and
 341 mutation for P_{j+1} to produce Q_{j+1} of size N , and;
- 342 5. the aforementioned steps are repeated until the convergence conditions are satisfied.

343 To clarify, the flow chart of Fig. 5 illustrates the entire method.

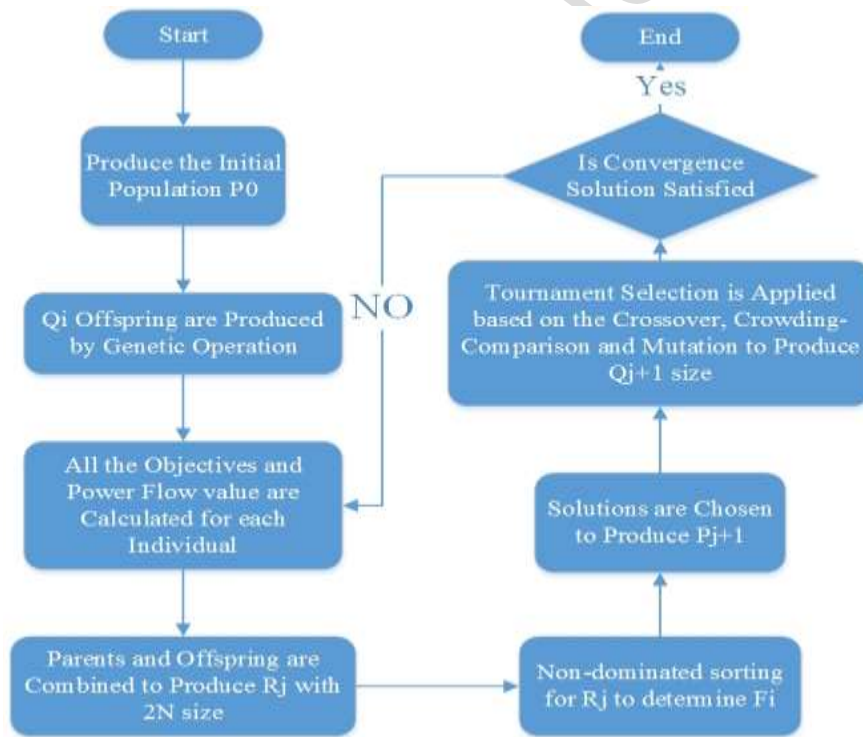


Figure 5. Flow chart of NSGA-II solving process.

3. Adaptive control; formulation, constraints and algorithm

347 Without properly controlling the supply and demand, it is difficult to achieve the desired task
 348 for the PSs, due to the inability of a conventional controller such as PID or PI types under a wide
 349 range of operations. Providing optimal coordination between EVs, PSs and HRESs requires a

350 new controller that can conform to the ideal situation in which the grid can be stable and power
351 losses can be reduced. In this regard, an adaptive charging and discharging controller is
352 described in this section, along with its formulations, algorithms and constraints.

353 **3.1. Constraints and formulation of optimal charging and discharging control**

354 As mentioned earlier, no less than 90% of the cars are parked during the day, providing an
355 opportunity to shift the electricity consumption from EV to times with lower demand, referred to
356 as G2V. This situation may also be employed for injecting power to the grid in order to flatten
357 the peak demand and to help regulate the grid frequency, referred to as V2G operation. It is
358 important to take into account energy requirements, which battery electric vehicle (BEV) owners
359 should meet, and which can be implemented in several ways by limiting the energy allowed for
360 use in V2G operation. In this way, it is guaranteed that the battery will not be completely
361 depleted. Nevertheless, based on the assumption for the BEV in this study, the missing energy in
362 the V2G condition could prevent the owners from making a trip, which is clearly not desirable.
363 Further, it has been demonstrated that the average distance traveled per day is approximately 40
364 km, which typically requires 8 kWh of electricity; this can be provided in 200 min at a rate of 2.4
365 kW [42]. Therefore, it is assumed that vehicles are not allowed to discharge to less than 8 kWh,
366 which is defined as “deep discharge” in this article. Providing exactly the same amount of power
367 to each (plug-in) electric vehicle is the most obvious and simple way to share the available active
368 power among EVs. Being adapted in a domestic charging scenario, it may be too complex and
369 unfair to allow higher or lower charging rates to some individual vehicles. Consequently, EVs
370 are considered to be charged or discharged at similar rates.

371 However, how frequently and at what times customers charge their vehicles determine
372 whether EVs help or harm the electricity infrastructure. Electrical energy storage for EVs can
373 play a prominent role in the electricity infrastructure with anticipated benefits encompassing
374 ancillary services, integrating renewable energy, and increasing the utility of the end user.
375 Accomplishing these objectives requires optimal coordination of EVs (charging and
376 discharging), PSs, and HRESs. The coordination of charging and discharging of EVs – which is
377 a demand response or demand side management application – illustrates the two pertinent
378 categories. Demand response is the underlying philosophy of these applications, as it aims to
379 adapt the power demand to the power generation applied to maintain the normal operation of the
380 electrical grid. One category is focused on charging and discharging decisions based on the

381 information of the state of the PS, and a second lies in forecasted estimation of the future power
 382 demand and the future state of the PS while making decisions about charging and discharging.

383 An objective function is utilized to provide a dataset that can be employed to minimize the
 384 total active power loss and to reduce the summation of voltage deviation. The objective function
 385 is expressed as follows:

$$\begin{aligned}
 \min f &= \min(P_{Loss}(u, v), V_{Deviation}(u, v)) \\
 g_i(u, v) &= 0 \\
 h_i(u, v) &\leq 0 \\
 u &= [x_1, \dots, x_{N_{vehicles}}] \\
 g_1 &= P_{DER}(t) + P_{Grid}(t) + \sum_{j=1}^{N_V} x_j(t)R - P_{Load}(t) - P_{Loss}(t) \\
 E_{StorageLimit-vehicle-i} &\leq E_{Storage}(t) \\
 E_{StorageLimit-vehicle-i} &= 8kWh \\
 V_{i-min} &\leq V(t) \leq V_{i-max} \\
 x_i(t) &\in \{-1, 0, 1\}
 \end{aligned} \tag{10}$$

386 Here, the vector $g_1(u, v) = 0$ represents equality constraints and is the load flow equation; the
 387 vector $h_1(u, v) \leq 0$ represents inequality constraints, such as the 8 kWh electric vehicle discharge
 388 threshold mentioned earlier; u is the controlling variables vector, which will be the output of the
 389 learning algorithm; and v is the vector of state variables.

390 3.2. Controller learning algorithms and system tuning configurations

391 Artificial intelligence-based controllers are widely used in industry, e.g., fuzzy, ANN, and
 392 ANFIS controllers. One problem with the conventional fuzzy controller is that its operation rules
 393 depend broadly on the knowledge and intuition of experts and the parameters associated with the
 394 membership functions. To overcome this problem, an adaptive neuro-fuzzy controller is
 395 proposed, which has advantages compared to conventional PI and PID controls and their
 396 adaptive versions. Due to the nonlinear and complicated nature of modern PSs, conventional
 397 control methods are not perfectly suitable for designing controllers which can cover a wide range
 398 of areas.

399 Neuro fuzzy techniques have emerged from the fusion of Artificial Neural Network (ANN)
 400 and Fuzzy Inference Systems (FIS) and have become popular for solving real-world problems. A

401 neuro fuzzy system is based on a fuzzy system, which is trained by a learning algorithm. Indeed,
402 an ANFIS-based controller can be trained without significant expert knowledge.

403 The adaptive controller in the present study is designed based on optimal power flow and
404 utilizes the Adoptive Neuro-Fuzzy inference System, which has exhibited well-known
405 advantages in the modeling and control of highly nonlinear systems [43].

406 Tuning the ANFIS structure involves adjusting all the modifiable parameters like values of
407 ANFIS rules and Gaussian membership function variables, which are generally $\{c_i, b_i, C_i, B_i\}$ and
408 $\{p_m, q_m, r_m\}$. Because of the random initial values for the controller, the procedures require
409 updating of the parameters, which may result in overestimations or underestimations. In this
410 regard, PSO as an evolutionary computational method is employed to tune the neuro fuzzy
411 system as derived from neural network theory.

412 The adaptive error PSO method updates the weights of the system for fast convergence of the
413 controller. The proposed controller, illustrated in Fig. 6, requires a set of data including inputs
414 and outputs to minimize the output error. Therefore, the optimal power flow (OPF) problem,
415 which was defined in the early 1960s to determine the optimal setting for control variables while
416 satisfying various constraints [44], is used here to provide the dataset of the optimal control
417 variables setting. The included control variables are $u = [x_1, \dots, x_{N_{vehicles}}]$ where x indicates
418 whether the BEV or PHEV must be charged, discharged or not exchange power by applying +1,
419 -1 and 0 values, respectively. The variable decisions are used for tuning the rules in the ANFIS
420 structures. Another most notable feature of the OPF problem is its applicability over a wide time
421 horizon. From the system operator perspective, the problem needs to be executed every 5
422 minutes, which is fixed in this study, to determine the optimal dispatch and to control the action
423 to be taken.

424 Training the ANFIS considering the data obtained, the system adjusts the parameters based on
425 the submitted inputs/outputs. The process of training continues only if the designated number of
426 times or the objective of the training error is reached. Moreover, a N-dimension vector is created,
427 where N represents the number of membership functions, which is optimized via the PSO
428 algorithm. The fitness function is defined as the mean square error.

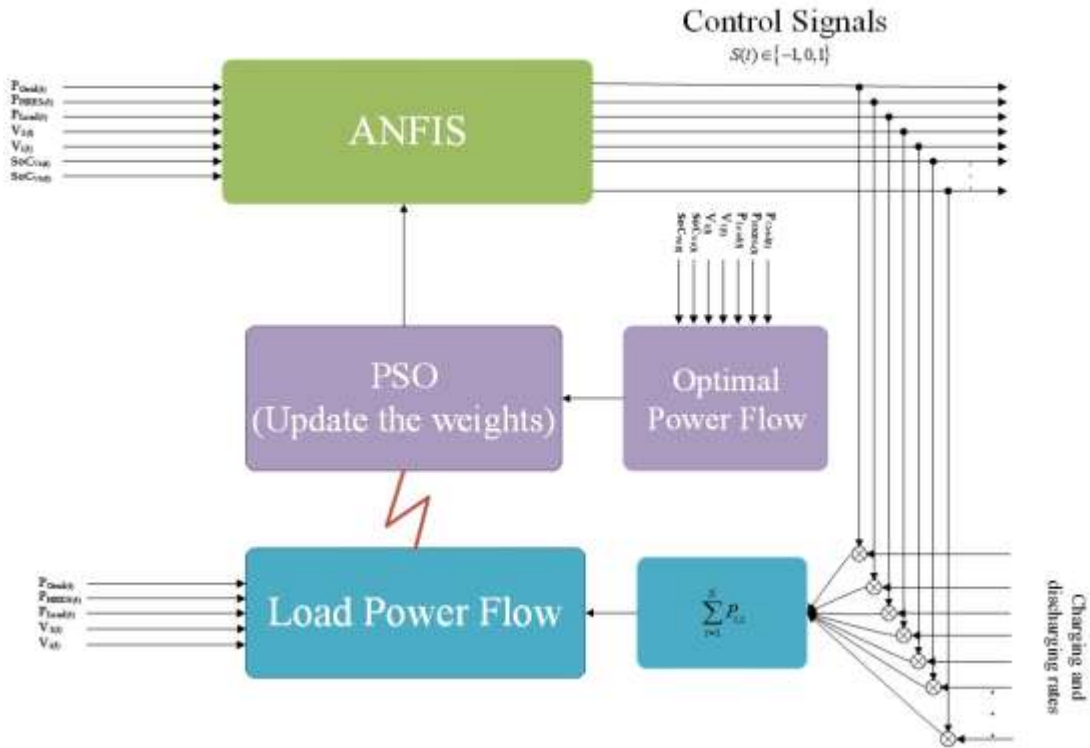


Figure 6. Proposed controller

429
430

431 In order to solve the single objective OPF problem, the objective functions presented earlier
432 are applied as a single objective in the optimization process on an IEEE-26 bus system.

433 The process of training can employ off- and on-line approaches. With the off-line approach,
434 the dataset does not include the full range of operating conditions, which may entail external
435 disturbances. Also, due to the uncertain behavior of PSs and BEVs, there are many unknown
436 conditions that may occur. To overcome these problems, a combination of on-line and off-line
437 training approaches is used. In many studies on SoC estimation, ANN and extended Kalman
438 filter approaches have been utilized [45]. These efforts demonstrate acceptable results once a
439 root mean square error of about 3% is achieved by the neural networks (NNs). The accuracy of
440 the NN model increases over time due to its adaptive and learning features. In addition, with
441 increasing in deployment of EVs, the availability of different types of data will increase and,
442 therefore, the model performance can improve. The modified PSO algorithm has been employed
443 to solve the single objective OPF problem. The modified PSO algorithm flowchart is presented
444 in Fig. 7.

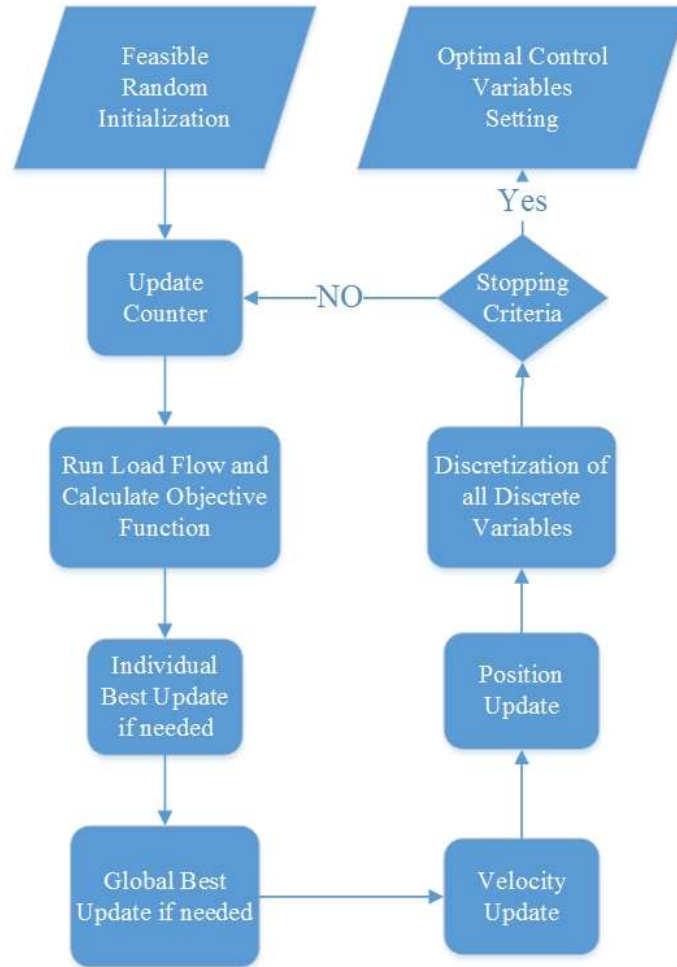


Figure 7. Single objective OPF algorithm using PSO algorithm

445

446

447 The PSO algorithm begins in an off-line mode to optimize the modifiable parameters of
 448 ANFIS based on the dataset. The proposed PSO initialization procedure is as follows:

449 Step 1: Initialize the PSO operators, the swarm size and the maximum number of iterations.

450 Step 2: Generate the initial swarm randomly, within certain bounds while each swarm contains
 451 the ANFIS controller's parameters such as Gaussian membership functions and rules
 452 $\{c_i, b_i, q_i\}$.

453 Step 3: Set the ANFIS initial parameter values $\{c_i, b_i, q_i\}$ for the PSO; they are used to calculate
 454 the mean square error.

455 Step 4: For each particle, update the P_{best} and G_{best} according to the cost value, which is the mean
 456 square error, and update each particle's velocity and position.

457 Step 5: Stop if the maximum number of generations is reached, otherwise increment the
 458 generations counter by one and go to step 3.

459 In total, the four aforementioned algorithms are integrated to develop the proposed controller
460 encompassing PSO, the modified OPF problem, the load flow and ANFIS, as shown in Fig. 7.

461 **4. Case study features**

462 Devices which are able to store electricity like BEVs can help the system to smooth the
463 intermittent behavior of renewable sources enabling easier integration. The non-deterministic
464 output is the main difference of parking lots as DGs and conventional DGs. The algorithm was
465 developed to provide net results for optimal placement and sizing of DGs. The peak loading
466 dataset of the test system is employed as typical load data.

467 In the implementation of the NSGA-II algorithm, the population number is 150, the maximum
468 iteration number is 250, and the crossover and mutation factors are both set to 1.5. The costs for
469 the PV and WT units are set to 2220 \$/kW and 720 \$/kW, respectively. The unit cost for
470 maintenance and operation of PVs and WTs is set to 0.015 \$/kWh. These values can be adjusted
471 according to the system and local distribution company under consideration.

472 The examined IEEE 26-bus system is depicted as a single line diagram in Fig. 8. The possible
473 candidate nodes for integrating parking lots as a DG system are nodes 6 to 25. Moreover, the
474 rated unit power is set to 15 kW for PV and 250 kW for WT, used to solve the OPF objective
475 function in the PSO algorithm.

476 **5. Results and discussion**

477 The results (see Table 2) demonstrate that the system s improves in terms of power loss and
478 voltage deviation reductions after integration of the optimally sized DGs into the studied grid.
479 The optimal multi-objective solution obtained out of sizing and siting problem considers voltage
480 profile, power losses and load characteristics of the busses besides V2G and G2V loads through
481 the grid to search for optimal location and number of units needed as summarized in Table 3. PV
482 and WT with 50 and 7 units, PV and WT with 117 and 10 units, PV and WT with 103 and 8
483 units located at node 14, 16 and 24, respectively. To consider the challenges of available load
484 near parking lots and to install WTs in real-world cases, besides the suitability of parking lot
485 structural issues, the maximum possible number of WT units can be restricted in the algorithm
486 (e.i. 10).

487

488

489

Table 2. System improvement after implementation of the optimally sized DGs into the system

System	Total active power load (MW)	Results before and after optimization			
			Annual DG I&O cost (\$)	Voltage deviation	Total active power losses (MW)
26-bus	1263	Before	0	17.6×10^2	14.337
		After	950×10^5	9.8×10^2	13.586

490

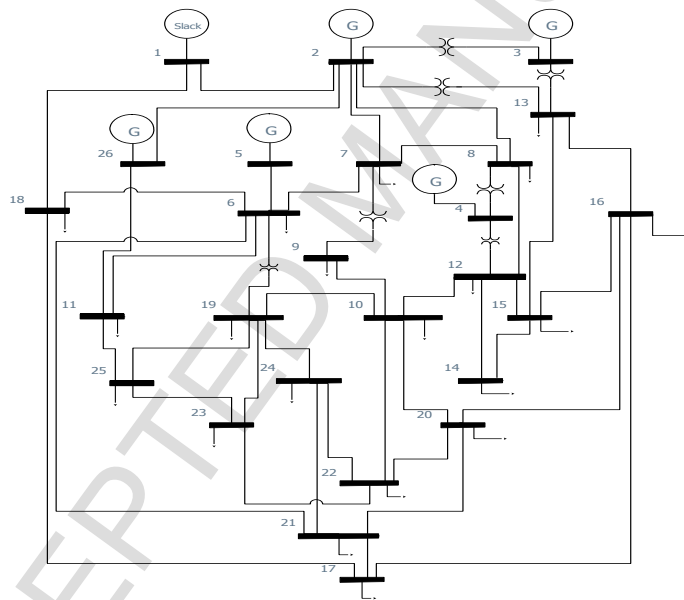
491

492

Table 3. Optimal sizing and sitting results

Node No.	No. of PV units	No. of WT units
14	50	7
16	117	10
24	103	8

493



494

495

Figure 8. Single line diagram of the test system

496

497

498

499

500

501

502

To verify the effectiveness and performance of the proposed PSO algorithm for solving the optimal power flow problem, and to assess the optimal values of PV buses over the time required in the next stage, objective functions were introduced to minimize a) the total active power loss, and b) the voltage deviation. As shown in Fig. 6 the optimal control values of $u = [P_{g1}, \dots, P_{gn}]$ can be determined via the PSO algorithm, so it is used to solve the objective OPF problem. The following parameters are used to enhance the algorithm's performance. The number of particles is set to 20, the acceleration factor including C_1 and C_2 are assumed to be 1.5, the inertia factor is

503 presumed to decrease linearly throughout each run, and the number of intervals N determining
 504 the maximum velocity V_k^{\max} is selected to be 8. The values of the objective function, P_{loss} , and the
 505 voltage deviation, for a standard 26-bus power system are listed in Table 4 and compared with
 506 Ref. [46]. Note in Table 4 that GSA refers to gravitational search algorithm.

507

508 **Table 3. Simulation results using GSA and PSO (26-bus system – after minimisation of voltage deviation and power loss)**

Objective	Minimization of voltage deviation [46]	Minimization of power loss [46]	Minimization of power loss and voltage deviation without considering DGs and parking lot	Minimization of power loss and voltage deviation considering DGs and parking lot (off peak)	Minimization of power loss and voltage deviation considering DGs and parking lot (on peak)
	GSA	GSA	PSO	PSO	PSO
P_{g1}	494.0021	451.7632	479.9778	100	426.4658
P_{g2}	199.6346	199.8991	200	50	164.7030
P_{g3}	171.7571	206.3199	180.2400	64.0185	2100
P_{g4}	147.7545	150	140	50	1600
P_{g5}	194.2034	180.7755	193	50	190.4443
P_{g14}	-	-	-	2.5	2.5000
P_{g16}	-	-	-	4.2300	4.2300
P_{g24}	-	-	-	3.5	3.5000
P_{g26}	69.6752	85.7769	80.8493	50	81.5117
V_1	1.0228	1.0500	1.0250	1.0250	1.0250
V_2	1.0225	1.0494	1.0200	1.0300	1.0200
V_3	1	1.0469	1.0350	1.0450	1.0350
V_4	1	1.0214	1.0600	1.0800	1.0600
V_5	1.0499	1.0499	1.0450	1.0550	1.0450
V_{14}	-	-	-	1.0300	1.0100
V_{16}	-	-	-	1.0300	0.9900
V_{24}	-	-	-	1.0300	0.9900
V_{26}	1.0069	1.0497	1.0150	1.0550	1.0150
OF	0.2534	0.1058	0.5858	0.1766	0.3105
P_{loss}	13.2551	10.5873	11.7460	2.6440	11.1070
SVD,	0.2534	0.6910	0.4684	0.15	0.3000
P_{dt}	1263	1263	1263	378.9000	1263

509

510 It can be observed from the Table 4 that, when the voltage deviation is considered as an
 511 objective function (OF) in the minimization mode, the power loss increases to 13.25 MW, and
 512 the summation of voltage deviation (SVD), which is a destructive characteristic of power quality,
 513 decreases to 0.25 (see columns 2 and 3). Nevertheless, as shown in column 3 where the power
 514 loss is considered as an OF, the inverse of the prior result is observed. The power loss decreased

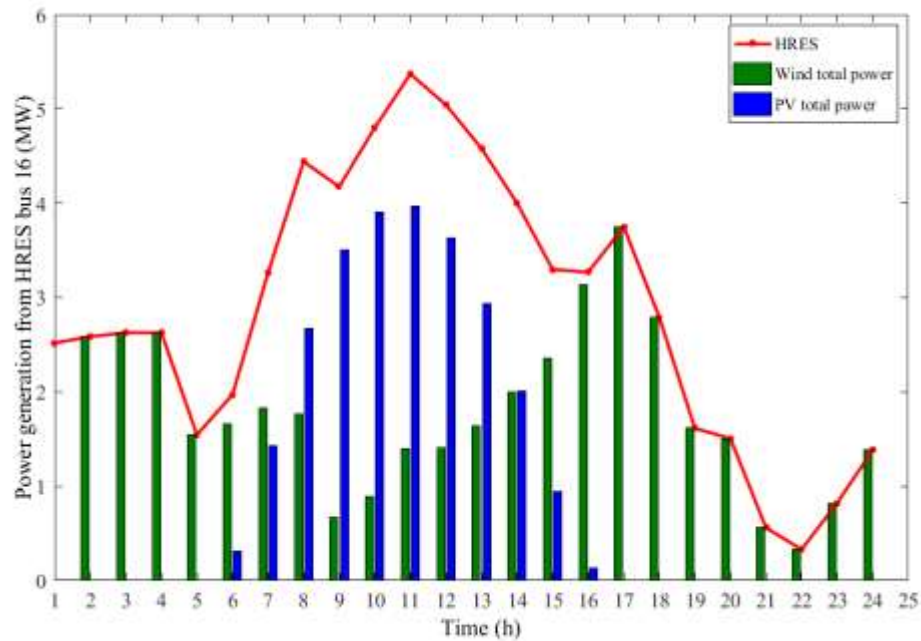
515 to 10.59 MW and the summation of the voltage deviation increased to 0.69. In addition, in
 516 columns 2, 3, 4 the effect of considering both of the OFs including power loss and voltage
 517 deviation can be identified. When the total active power loss is reduced to 11.75 MW from 13.25
 518 MW, the total active power loss is increased to 11.75 from 10.59, as can be seen in column 2,
 519 because both voltage deviation and active power loss are considered as the objective. Moreover,
 520 the summation of the voltage deviation is increased to 0.47 from 0.25; but it is reduced to 0.47
 521 from 0.69 when both the power loss and voltage deviation are identified as the objective.

522 Consequently, combining the power loss and the voltage deviation as the OFs in an
 523 optimization process demonstrates that the proposed OPF algorithm is able to manage both
 524 values in a positive way. With the assumption of constant power generation by a HRES at off-
 525 peak and on peak periods, the problem is resolved. Accordingly, the results indicate that the
 526 power loss and the summation of the voltage deviation for on peak periods are reduced to 11.11
 527 MW from 11.75 MW and to 0.30 from 0.47, respectively. Nonetheless, the intermittent behavior
 528 of an HRES is worth considering; therefore, the output of the PV and WT units is subject to the
 529 achievable power patterns of irradiation and wind velocity data, which were illustrated in Figs. 4
 530 and 5. The transition from verification and obtaining the variable decisions, the control vector of
 531 the optimal power flow problem is rewritten as $u = [x_{1,t}, \dots, x_{N_{vehicles},t}]$ and the state of charge of
 532 the electric vehicles arrived at for the previous time is obtained from the state of the vector,
 533 which is formulated as $v = [SoC_{1,t}, \dots, SoC_{N,t}]$. Notably, the objective of the OPF problem is to
 534 determine the setting of the control variables with broad aims, such as reactive power output of
 535 different reactive power sources, the active and reactive power generation at power plants, the
 536 on-load tap charging transformer tap position, etc. [46].

537 The arrival and departure times are created randomly. The former are generated between 6:00
 538 AM to 11:59 PM, and the minimum departure times of BEVs are considered to be 30 minutes.
 539 The OPF introduced previously has been run on a core i-7 computer with 4G DRR3 RAM and
 540 CPU 1.73 GHz in MATLAB[®]. Further, the parameters of the PSO algorithm in this step are the
 541 same as previously given. The design capacity of the parking lot located on bus 16 is 300 electric
 542 vehicles. Moreover, the capacity of EV batteries generally ranges from 20 to 85 kWh in this
 543 study, therefore, the capacity of EVs for simulation is considered to be 50 kWh, 100 Ah. Note
 544 that the battery parameters and associated characteristics vary with respect to the type of the
 545 battery and its manufacturer.

546 The modified OPF problem begins using random data regarding the EV departure and arrival
547 times from 6 AM to 11:59 PM, with run time intervals set to five minutes. The power generation
548 from the power plants encompassing P_1 to P_5 and P_{26} are fixed from the previous step and remain
549 constant during the estimation of the modified controlling vector related to the EVs. As shown in
550 Appendix A, during the time interval 6 AM-7 AM, 37 EVs arrive at the parking lot, and
551 approximately 23 of them have energy contents between 2 kWh to 30 kWh. On the supply side,
552 the power generation by the HRES is 1.97 MW on bus 16. The results related to this interval
553 indicate that 18, 19 and 0 EVs are charged, kept on standby and discharged when the irradiation
554 and wind velocity are 100 W/m^2 and 4 m/s, respectively. In addition, during this interval, the
555 status of the five EVs that were on standby in the previous step changed their status to charging.
556 The energy stored from 6 AM-7 AM is increased to 0.92 MWh from 0.85 MWh. As the power
557 generation increases to 3.26 MW from 1.97 MW and simultaneously the load demand steadily
558 increases to 36 MW, and the number of EVs increases to 75, Among these, 38 EVs are plugged
559 in between 7 AM-8 AM such that 20, 15 and 3 of them are charged, held on standby and
560 discharged. The number of EVs remaining in the charged and standby statuses from the prior
561 interval are 28 and 9, respectively. The EVs with IDs 64, 65, and 66 discharge in 20 minutes. In
562 third time interval from 8 AM to 9 AM, 9 EVs with IDs 3, 4, 31, 33, 39, 40, 62, 63, and 92
563 departed from parking with their energy increased to 23.8, 9.8, 21.8, 32, 27.8, 8.8, 15.8, 14.8,
564 and 30 kWh, while EVs with IDs 3, 4, 40, and 63 were plugged in all the time.

565 Fig. 9 illustrates the power generated by the components sized for the HRES of bus 16 over
566 24 h. As can be seen, the PV modules supply electricity to the grid at 6 AM-4 PM and most of
567 the electricity via the generic WTs is supplied between 2 PM-8 PM and 1 AM-4 AM owing to
568 higher presence of the wind energy density and the received solar radiation in these time ranges.
569 Also, the lowest solar generation occurs between 5 PM-11.59 PM and 1 AM-5 AM.

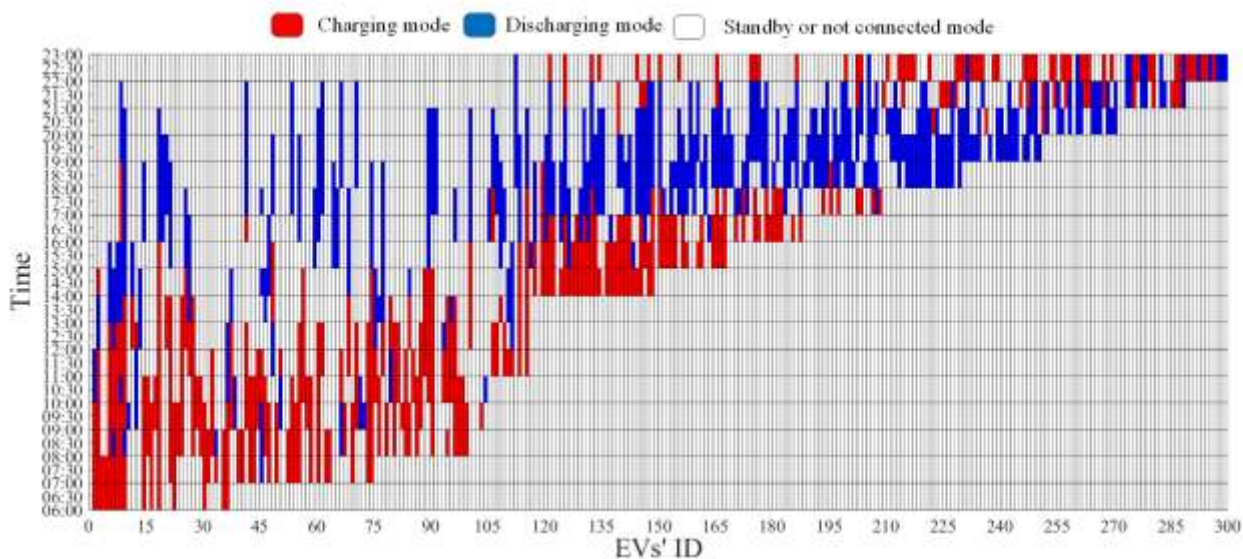


570

571

Figure 9. Simulation of optimal result of HRES bus 16

572 The results of the modified OPF problem control vector are depicted as a contour plot, which
 573 is a graphical technique to represent a 3 dimensional surface while the data do not form a regular
 574 grid, that indicates the state of the EVs as a function of time. According to Fig. 10, the X and Y
 575 axes are related to the EVs' ID and time, and the three color spectrums of red, white, and blue
 576 represent the charging, standby or not connected and discharging states, i.e., 1, 0, -1,
 577 respectively.

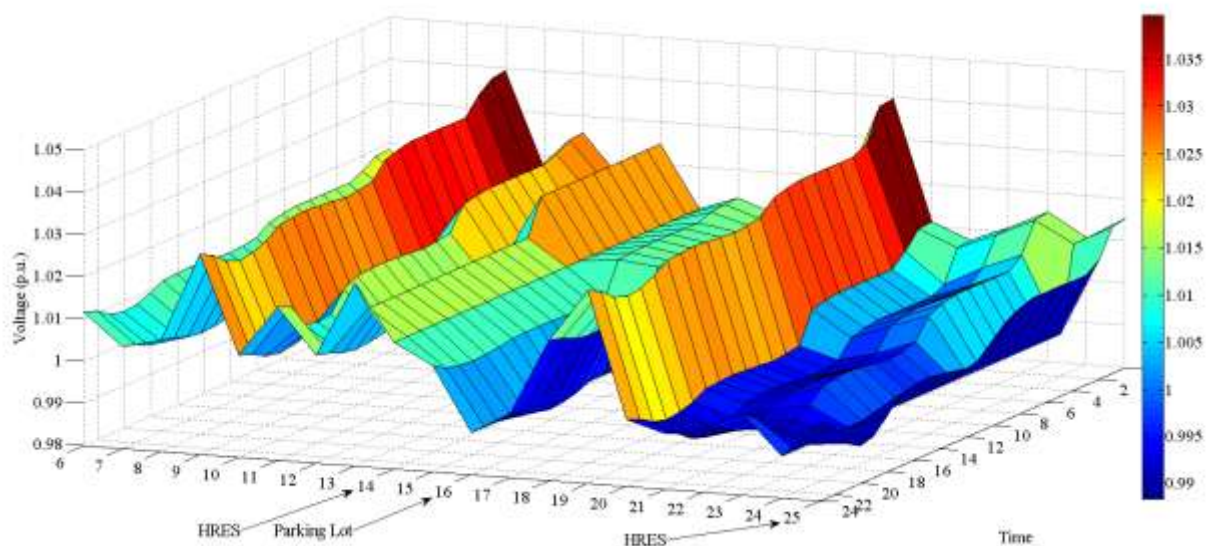


578

579

Figure 10. Charging and discharging results for the OPF problem

580 The plot in Fig. 10 is divided into two areas. The first between 6 AM-4 PM when the
 581 electricity generation via renewable energy is high and the load demand is low; therefore, a high
 582 portion of EVs are charged in this period. Nevertheless, owing to the fluctuation of renewable
 583 energy resources, some of the EVs are discharged in this time. The second area occurs from 4
 584 PM-10 PM when load demand is a maximum. Hence, as peak demand and the HRES power
 585 generation reduction occur in this period, a high number of EVs are discharged in this time. The
 586 minimum and maximum energy storages of EVs (14 kWh and 49 kWh) demonstrate that all
 587 vehicles satisfy the formerly stated constraints.



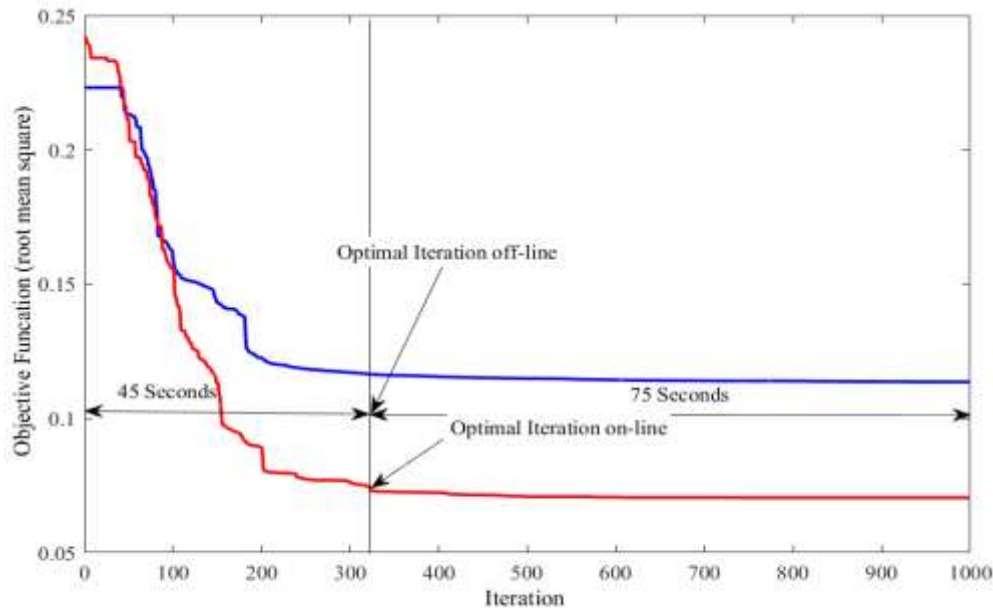
588

589

Figure 11. Time-based Voltage profile through the buses

590 Fig. 11 shows the voltage profile for buses, which demonstrates the stability of the system
 591 within the desired per unit defined range. The obtained results are utilized to tune the real time
 592 controller (PSO-ANFIS), and the main advantage of the proposed controller as mentioned earlier
 593 is being adaptive and making the system responsible for different contingencies.

594 Model verification is based on the data in Appendix A. Reference [47] presents arrival and
 595 departure times of vehicles and initial energy contents. In addition, the wind velocity and
 596 irradiation data used to calculate power generation are obtained for the date, February 2nd as
 597 design data. Note that the total active power loss and voltage deviation are considered throughout
 598 the entire charging and discharging. If at any time the load flow and the voltage deviation violate
 599 a constraint (e.g. voltage out of limits) at any node, the load flow algorithm sets zero values in
 600 the controller outputs, which indicates a standby status; the controller will be tuned again by the
 601 data collected and provided via a modified OPF. The reason for using the proposed controller
 602 instead of a modified OPF is its real-time functionality for EVs. The modified OPF is run at 5
 603 minute steps; therefore, it is unlikely to be used instead of the proposed controller.



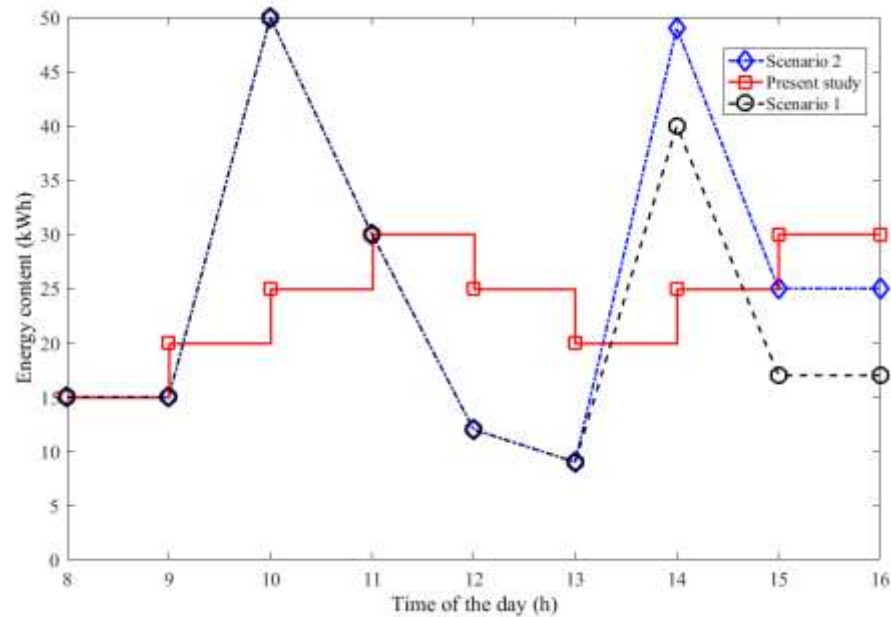
604

605

Figure 12. Number of iterations for convergence of controller

606 Fig. 12 shows the number of required iterations for achieving convergence, which is obtained
 607 via trial and error. Tuning modifiable ANFIS parameters takes 45 seconds for the off-line and
 608 on-line methods.

609 Despite the differences between the objective functions of the present study and [47], there are
 610 some structural similarities between the two studies. In reference [47], the proposed model
 611 optimally charges and discharges the EVs based on avoiding overload in the distribution system
 612 and the technical and economic preferences of owners. EVs are charged during time periods of
 613 low electricity prices and they are discharged at high price time periods; charging and
 614 discharging prices are associated with off-peak and on-peak periods, respectively. Therefore, the
 615 net results of the present study with the aforementioned reference are compared.



616

617

Figure 13. Comparison of the 75th EV's Energy content in reference 59 and the present study

618 With regard to [47], the charging and discharging of the 75th vehicle are marked with stars
 619 and circle symbols in Fig. 13. As can be seen, from 9-10 AM, the energy content is increased
 620 from 15 kWh to 50 kWh, showing that the battery was charged at the maximum charging rate
 621 and that, after 3 hours, the energy level is dramatically decreased by 41 kWh from 50 kWh to 9
 622 kWh which is not favorable from battery life point of view. Hence, the battery experiences a
 623 significant deep discharge rate in scenarios taken from the literature compared to the present
 624 study which exhibits a steadier trend. In addition, at the end of the whole charging and
 625 discharging processes, the proposed controller charged the vehicle by 30 kWh and outperformed
 626 compared to scenarios 1 and 2 which charged the same vehicle to 17 and 25 kWh, respectively.
 627 Based on the time-energy content plot for the present study in the first cycle, the battery was
 628 charged 30 kWh because of considering the state of the grid, the HRES, and the 75th vehicle's

629 SoC. Then, the controller will discharge to around 20 kWh, demonstrating that the controller
630 prevented the vehicle from reaching the point which were defined as deep discharge state in the
631 proposed algorithm. It should be taken into consideration that the energy flow exchanged via
632 scenarios 1 and 2 are higher compared to the present study.

633 **6. Conclusions**

634 This study not only used an intelligent NSGA optimization approach for optimal sizing and
635 siting of distribution generation systems, but also presented a real-time PSO-based controller
636 with an adaptive neuro-fuzzy inference system toward optimal integrating of renewable energy
637 sources (wind and solar) and EVs into a smart grid infrastructure.

638 In order to integrate EVs and reduce the fluctuation of renewable DG outputs, a robust control
639 method was introduced and developed to tackle efficiently an optimal power flow problem
640 allowing G2V and V2G functionalities and addressing deep discharging challenges. This method
641 was compared to others reported in the literature. In addition, the proposed approach could
642 exhibit techno-economic capabilities in offering ancillary services such as power leveraging,
643 voltage regulation, and power system operating cost reduction to the studied PS while having
644 EVs as a system component. Hence the study offered a real-time and intelligent control approach
645 to provide beneficial options and opportunities for grid-friendly deployment of EVs in smart grid
646 systems. Nevertheless, the following limitations need to be addressed in future studies:

- 647 1- As the great proportion of objectives of such studies focus on economic aspects, further
648 investigations are merited on other technical aspects (e.g. frequency deviation and
649 harmonic distortions).
- 650 2- Since a reduction in the voltage deviation generally leads to an increase in the total
651 harmonic distortion of voltage, such factors should be considered as targets in weighted
652 multi-objective functions.
- 653 3- In addition to the proposed multi-objective problem for improving the grid stability, the
654 influence of EV discharging and charging rates, which are fixed in this study, need to be
655 assessed.
- 656 4- Although battery state of health plays a prominent role in V2G concepts, it is not
657 considered in the present study due to the inherent complexity of doing so, but this value
658 should be considered as a direct signal in future work, leading to further computational
659 cost and inputs. The present authors are starting to address this issue by data fusion

660 processes. However, it was predicted that by considering these parameters, EVs are not
661 capable to provide desirable energy for V2G services because of the high battery
662 degradation costs corresponding to V2G cycling.

663 5- EVs chargers are based on assumption of off-board placement, which raise concerns about
664 battery heating management and their capability with other charging stations, and further
665 information about this is required.

666 References

- 667 [1] Iqbal M, Azam M, Naeem M, Khwaja AS, Anpalagan A. Optimization classification, algorithms and
668 tools for renewable energy: A review. *Renewable and Sustainable Energy Reviews*. 2014;39:640-54.
- 669 [2] Mwasilu F, Justo JJ, Kim E-K, Do TD, Jung J-W. Electric vehicles and smart grid interaction: A review on
670 vehicle to grid and renewable energy sources integration. *Renewable and Sustainable Energy Reviews*.
671 2014;34:501-16.
- 672 [3] Stevanović S. Optimization of passive solar design strategies: A review. *Renewable and Sustainable*
673 *Energy Reviews*. 2013;25:177-96.
- 674 [4] Fazelpour F, Vafaeipour M, Rahbari O, Rosen MA. Intelligent optimization to integrate a plug-in
675 hybrid electric vehicle smart parking lot with renewable energy resources and enhance grid
676 characteristics. *Energy Conversion and Management*. 2014;77:250-61.
- 677 [5] Rahbari O, Vafaeipour M, Fazelpour F, Feidt M, Rosen MA. Towards realistic designs of wind farm
678 layouts: Application of a novel placement selector approach. *Energy Conversion and Management*.
679 2014;81:242-54.
- 680 [6] Delfino F, Bracco S, Pampararo F. 2 - Key performance indicators in assessing new technology
681 for electricity transmission and distribution networks. In: Bessède J-L, editor. *Eco-Friendly Innovation in*
682 *Electricity Transmission and Distribution Networks*. Oxford: Woodhead Publishing; 2015. p. 47-63.
- 683 [7] Bouhouras AS, Labridis DP. Influence of load alterations to optimal network configuration for loss
684 reduction. *Electric Power Systems Research*. 2012;86:17-27.
- 685 [8] Battistelli C, Baringo L, Conejo AJ. Optimal energy management of small electric energy systems
686 including V2G facilities and renewable energy sources. *Electric Power Systems Research*. 2012;92:50-9.
- 687 [9] Fazelpour F, Vafaeipour M, Rahbari O, Rosen MA. Intelligent optimization of charge allocation for
688 plug-in hybrid electric vehicles utilizing renewable energy considering grid characteristics. *Smart Energy*
689 *Grid Engineering (SEGE)*, 2013 IEEE International Conference on 2013. p. 1-8.
- 690 [10] Da Qian X, Joos G, Levesque M, Maier M. Integrated V2G, G2V, and Renewable Energy Sources
691 Coordination Over a Converged Fiber-Wireless Broadband Access Network. *Smart Grid, IEEE*
692 *Transactions on*. 2013;4:1381-90.
- 693 [11] Moradijoz M, Parsa Moghaddam M, Haghifam MR, Alishahi E. A multi-objective optimization
694 problem for allocating parking lots in a distribution network. *International Journal of Electrical Power &*
695 *Energy Systems*. 2013;46:115-22.
- 696 [12] Yu X, Cecati C, Dillon T, Simoes MG. The new frontier of smart grids. *IEEE Industrial Electronics*
697 *Magazine*. 2011;5:49-63.
- 698 [13] Shaaban MF, Atwa YM, El-Saadany EF. DG allocation for benefit maximization in distribution
699 networks. *IEEE Transactions on Power Systems*. 2013;28:639-49.
- 700 [14] Ferruzzi G, Graditi G, Rossi F, Russo A. Optimal operation of a residential microgrid: The role of
701 demand side management. *Intelligent Industrial Systems*. 2015;1:61-82.

- 702 [15] Vasirani M, Kota R, Cavalcante RL, Ossowski S, Jennings NR. An agent-based approach to virtual
703 power plants of wind power generators and electric vehicles. *IEEE Transactions on Smart Grid*.
704 2013;4:1314-22.
- 705 [16] Falvo MC, Graditi G, Siano P. Electric vehicles integration in demand response programs. *Power*
706 *Electronics, Electrical Drives, Automation and Motion (SPEEDAM)*, 2014 International Symposium on:
707 IEEE; 2014. p. 548-53.
- 708 [17] López M, De La Torre S, Martín S, Aguado J. Demand-side management in smart grid operation
709 considering electric vehicles load shifting and vehicle-to-grid support. *International Journal of Electrical*
710 *Power & Energy Systems*. 2015;64:689-98.
- 711 [18] Sovacool BK, Hirsh RF. Beyond batteries: An examination of the benefits and barriers to plug-in
712 hybrid electric vehicles (PHEVs) and a vehicle-to-grid (V2G) transition. *Energy Policy*. 2009;37:1095-103.
- 713 [19] Graditi G, Ippolito M, Telaretti E, Zizzo G. Technical and economical assessment of distributed
714 electrochemical storages for load shifting applications: An Italian case study. *Renewable and Sustainable*
715 *Energy Reviews*. 2016;57:515-23.
- 716 [20] Rahimi-Eichi H, Ojha U, Baronti F, Chow M-Y. Battery management system: An overview of its
717 application in the smart grid and electric vehicles. *IEEE Industrial Electronics Magazine*. 2013;7:4-16.
- 718 [21] Di Silvestre ML, Sanseverino ER, Zizzo G, Graditi G. An optimization approach for efficient
719 management of EV parking lots with batteries recharging facilities. *Journal of Ambient Intelligence and*
720 *Humanized Computing*. 2013;4:641-9.
- 721 [22] Tie SF, Tan CW. A review of energy sources and energy management system in electric vehicles.
722 *Renewable and Sustainable Energy Reviews*. 2013;20:82-102.
- 723 [23] Omar N, Daowd M, Bossche Pvd, Hegazy O, Smekens J, Coosemans T, et al. Rechargeable Energy
724 Storage Systems for Plug-in Hybrid Electric Vehicles—Assessment of Electrical Characteristics. *Energies*.
725 2012;5:2952-88.
- 726 [24] Omar N, Monem MA, Firouz Y, Salminen J, Smekens J, Hegazy O, et al. Lithium iron phosphate
727 based battery – Assessment of the aging parameters and development of cycle life model. *Applied*
728 *Energy*. 2014;113:1575-85.
- 729 [25] Waraich RA, Galus MD, Dobler C, Balmer M, Andersson G, Axhausen KW. Plug-in hybrid electric
730 vehicles and smart grids: Investigations based on a microsimulation. *Transportation Research Part C:*
731 *Emerging Technologies*. 2013;28:74-86.
- 732 [26] Haider AM, Muttaqi KM, Sutanto D. Technical challenges for electric power industries due to grid-
733 integrated electric vehicles in low voltage distributions. A review by published in *Energy conversion and*
734 *management Elsevier*. 2014;86:689-700.
- 735 [27] Young-Min W, Jong-uk L, Sung-Kwan J. Electric vehicle charging method for smart homes/buildings
736 with a photovoltaic system. *Consumer Electronics, IEEE Transactions on*. 2013;59:323-8.
- 737 [28] Tan M, Mohamed A, Mohammed O. Optimal charging of plug-in electric vehicles for a car park
738 infrastructure. *Industry Applications Society Annual Meeting (IAS), 2012 IEEE2012*. p. 1-8.
- 739 [29] Pillai JR, Bak-Jensen B. Integration of Vehicle-to-Grid in the Western Danish Power System.
740 *Sustainable Energy, IEEE Transactions on*. 2011;2:12-9.
- 741 [30] Singh M, Kar I, Kumar P. Influence of EV on grid power quality and optimizing the charging schedule
742 to mitigate voltage imbalance and reduce power loss. *Power Electronics and Motion Control*
743 *Conference (EPE/PEMC), 2010 14th International2010*. p. T2-196-T2-203.
- 744 [31] Kaushal A, Verma N. Implementation of vehicle to grid concept using ANN and ANFIS controller.
745 *Industrial Electronics and Applications (ICIEA), 2014 IEEE 9th Conference on2014*. p. 960-5.
- 746 [32] Masoum AS, Deilami S, Moses PS, Masoum MAS, Abu-Siada A. Smart load management of plug-in
747 electric vehicles in distribution and residential networks with charging stations for peak shaving and loss
748 minimisation considering voltage regulation. *IET Generation, Transmission & Distribution*. 2011;5:877-
749 88.

- 750 [33] Deilami S, Masoum AS, Moses PS, Masoum MAS. Real-Time Coordination of Plug-In Electric Vehicle
751 Charging in Smart Grids to Minimize Power Losses and Improve Voltage Profile. *IEEE Transactions on*
752 *Smart Grid*. 2011;2:456-67.
- 753 [34] Singh M, Kumar P, Kar I. Implementation of Vehicle to Grid Infrastructure Using Fuzzy Logic
754 Controller. *IEEE Transactions on Smart Grid*. 2012;3:565-77.
- 755 [35] Nguyen HNT, Zhang C, Mahmud MA. Optimal Coordination of G2V and V2G to Support Power Grids
756 With High Penetration of Renewable Energy. *IEEE Transactions on Transportation Electrification*.
757 2015;1:188-95.
- 758 [36] Liu K-y, Sheng W, Liu Y, Meng X, Liu Y. Optimal sitting and sizing of DGs in distribution system
759 considering time sequence characteristics of loads and DGs. *International Journal of Electrical Power &*
760 *Energy Systems*. 2015;69:430-40.
- 761 [37] Lin X, Sun J, Ai S, Xiong X, Wan Y, Yang D. Distribution network planning integrating charging
762 stations of electric vehicle with V2G. *International Journal of Electrical Power & Energy Systems*.
763 2014;63:507-12.
- 764 [38] Srinivas N, Deb K. Multiobjective optimization using nondominated sorting in genetic algorithms.
765 *Evolutionary computation*. 1994;2:221-48.
- 766 [39] Ramaswamy PC, Deconinck G. Smart grid reconfiguration using simple genetic algorithm and NSGA-
767 II. *Innovative Smart Grid Technologies (ISGT Europe), 2012 3rd IEEE PES International Conference and*
768 *Exhibition on: IEEE; 2012*. p. 1-8.
- 769 [40] Zamanifar M, Fani B, Golshan MEH, Karshenas HR. Dynamic modeling and optimal control of DFIG
770 wind energy systems using DFT and NSGA-II. *Electric Power Systems Research*. 2014;108:50-8.
- 771 [41] Van Veldhuizen DA, Lamont GB. Multiobjective evolutionary algorithms: Analyzing the state-of-the-
772 art. *Evolutionary computation*. 2000;8:125-47.
- 773 [42] de Hoog J, Alpcan T, Brazil M, Thomas DA, Mareels I. Optimal Charging of Electric Vehicles Taking
774 Distribution Network Constraints Into Account. *Power Systems, IEEE Transactions on*. 2015;30:365-75.
- 775 [43] Singh M, Chandra A. Real-Time Implementation of ANFIS Control for Renewable Interfacing Inverter
776 in 3P4W Distribution Network. *Industrial Electronics, IEEE Transactions on*. 2013;60:121-8.
- 777 [44] Bhattacharya K, Bollen, Math, Daalder, Jaap E. Operation of Restructured Power Systems 2001.
- 778 [45] Charkhgard M, Farrokhi M. State-of-Charge Estimation for Lithium-Ion Batteries Using Neural
779 Networks and EKF. *Industrial Electronics, IEEE Transactions on*. 2010;57:4178-87.
- 780 [46] Bhattacharya A, Roy PK. Solution of multi-objective optimal power flow using gravitational search
781 algorithm. *Generation, Transmission & Distribution, IET*. 2012;6:751-63.
- 782 [47] Mirzaei MJ, Kazemi A, Homaei O. Real-world based approach for optimal management of electric
783 vehicles in an intelligent parking lot considering simultaneous satisfaction of vehicle owners and parking
784 operator. *Energy*. 2014;76:345-56.

785

786

Appendix A

Table A.1

Data on electric vehicles

Vehicle no.	Arrival time	Departure time	Initial SoC	Vehicle no.	Arrival time	Departure time	Initial SoC	Vehicle no.	Arrival time	Departure time	Initial SoC
1	6:00	12:00	26	101	9:00	9:30	30	201	17:33	19:54	28
2	6:00	15:00	9	102	9:05	10:50	30	202	17:36	22:47	21
3	6:00	8:00	19	103	9:10	12:50	32	203	17:39	22:33	21
4	6:00	8:00	5	104	10:00	11:00	38	204	17:42	18:30	48
5	6:00	16:00	10	105	10:05	17:30	43	205	17:45	23:27	50
6	6:05	15:00	44	106	11:00	20:30	26	206	17:48	22:00	33
7	6:05	15:50	8	107	11:05	19:45	36	207	17:51	21:20	47
8	6:05	21:05	19	108	11:10	18:30	43	208	17:54	20:23	25
9	6:05	20:10	44	109	11:10	17:50	33	209	17:57	21:20	14
10	6:10	9:10	43	110	11:15	14:50	41	210	18:00	23:00	17
11	6:10	15:35	35	111	11:15	16:00	42	211	18:03	21:45	34
12	6:10	12:25	44	112	11:20	23:05	45	212	18:06	22:00	37
13	6:15	14:20	44	113	11:30	19:40	23	213	18:09	22:30	37
14	6:15	18:45	24	114	11:30	15:30	30	214	18:12	22:36	10
15	6:20	12:55	23	115	11:35	20:40	1	215	18:15	23:55	30
16	6:20	9:35	18	116	11:40	16:05	30	216	18:18	23:47	17
17	6:20	10:15	28	117	12:00	18:35	30	217	18:21	22:30	38
18	6:20	20:30	2	118	12:10	15:25	27	218	18:24	21:00	48
19	6:25	19:45	47	119	14:00	21:20	3	219	18:27	23:55	42
20	6:25	19:05	33	120	14:00	19:35	30	220	18:30	22:41	50
21	6:30	18:30	7	121	14:05	23:15	24	221	18:33	23:55	30
22	6:30	13:00	12	122	14:05	18:30	9	222	18:36	20:35	12
23	6:30	12:35	26	123	14:25	15:30	20	223	18:39	21:00	48
24	6:30	16:15	6	124	14:25	19:00	47	224	18:42	21:50	20
25	6:35	15:30	30	125	14:30	22:18	13	225	18:45	21:55	25
26	6:35	17:25	40	126	14:30	16:10	41	226	18:48	22:00	25
27	6:35	14:00	6	127	14:30	15:55	10	227	18:51	22:05	47
28	6:35	11:30	35	128	14:30	16:35	10	228	18:54	22:10	15
29	6:40	10:55	9	129	14:30	18:00	21	229	18:57	22:15	27
30	6:45	9:40	9	130	14:30	20:35	23	230	19:00	22:45	29
31	6:45	8:50	17	131	14:30	18:40	37	231	19:03	22:41	50
32	6:45	13:30	14	132	14:30	22:40	13	232	19:06	20:20	24
33	6:50	8:10	32	133	14:30	19:35	18	233	19:09	22:30	18
34	6:50	9:20	31	134	14:30	23:10	44	234	19:12	23:17	26
35	6:55	10:15	15	135	14:30	21:00	35	235	19:15	23:38	16
36	6:55	13:00	18	136	14:30	15:30	7	236	19:18	20:50	12
37	6:55	16:15	21	137	14:30	17:00	19	237	19:21	19:34	34

38	7:00	10:55	38	138	14:30	16:00	8	238	19:24	23:55	19
39	7:00	8:50	23	139	14:30	22:10	5	239	19:27	22:42	31
40	7:00	8:10	4	140	14:30	19:15	2	240	19:30	21:30	38
41	7:00	21:10	20	141	14:35	16:53	18	241	19:33	21:35	29
42	7:05	12:20	5	142	14:35	19:40	30	242	19:36	21:40	40
43	7:05	11:15	6	143	14:40	15:50	33	243	19:39	21:45	40
44	7:05	13:30	21	144	14:40	22:12	43	244	19:42	21:50	43
45	7:10	17:25	38	145	14:45	21:35	21	245	19:45	21:55	11
46	7:10	14:35	20	146	14:48	21:37	45	246	19:48	23:34	13
47	7:10	16:05	26	147	14:51	23:47	35	247	19:51	23:00	29
48	7:15	19:40	35	148	14:54	21:50	26	248	19:54	23:00	27
49	7:15	9:55	11	149	14:57	16:40	30	249	19:57	23:30	47
50	7:20	13:45	31	150	15:00	22:32	27	250	20:00	20:45	33
51	7:20	11:05	32	151	15:03	17:40	21	251	20:03	22:00	14
52	7:25	11:10	22	152	15:06	16:42	19	252	20:06	21:50	40
53	7:25	21:40	26	153	15:09	18:20	26	253	20:09	23:55	13
54	7:25	9:10	11	154	15:12	18:21	11	254	20:12	22:18	13
55	7:25	19:40	15	155	15:15	23:46	32	255	20:15	22:49	38
56	7:30	14:50	3	156	15:18	19:34	22	256	20:18	22:30	36
57	7:30	10:15	21	157	15:21	18:11	25	257	20:21	22:35	16
58	7:30	10:20	1	158	15:24	22:39	50	258	20:24	22:40	31
59	7:35	17:30	39	159	15:27	19:25	48	259	20:27	22:45	28
60	7:35	20:40	15	160	15:30	21:30	45	260	20:30	22:50	40
61	7:00	21:20	36	161	15:33	18:49	12	261	20:33	22:55	32
62	7:40	8:55	11	162	15:36	19:11	47	262	20:36	23:00	13
63	7:45	8:45	10	163	15:39	16:55	29	263	20:39	23:50	11
64	7:45	18:55	45	164	15:42	20:49	36	264	20:42	22:00	49
65	7:45	17:20	44	165	15:45	23:14	17	265	20:45	23:55	28
66	7:45	21:10	46	166	15:48	21:32	38	266	20:48	23:00	47
67	7:45	10:00	21	167	15:51	19:50	15	267	20:51	23:10	15
68	7:50	17:30	34	168	15:54	20:12	47	268	20:54	22:30	40
69	7:50	9:30	10	169	15:57	19:26	33	269	20:57	23:43	18
70	7:50	23:00	27	170	16:00	17:34	27	270	21:00	23:55	38
71	7:50	10:20	37	171	16:03	19:20	36	271	21:03	21:45	19
72	7:55	9:30	40	172	16:06	18:40	24	272	21:06	22:00	29
73	7:55	12:52	2	173	16:09	19:10	46	273	21:09	22:30	49
74	7:55	18:30	8	174	16:12	23:25	31	274	21:12	23:10	50
75	7:55	14:15	40	175	16:15	23:25	25	275	21:15	23:08	10
76	8:00	13:30	18	176	16:18	23:34	25	276	21:18	23:55	20
77	8:00	18:40	44	177	16:21	23:55	35	277	21:21	22:40	49
78	8:00	9:45	10	178	16:24	22:50	34	278	21:24	22:45	48
79	8:00	15:28	33	179	16:27	17:30	21	279	21:27	23:50	21
80	8:00	14:25	9	180	16:30	18:35	17	280	21:30	23:55	12

81	8:00	12:20	12	181	16:33	22:24	20	281	21:33	23:55	26
82	8:00	9:10	18	182	16:36	17:40	18	282	21:36	22:40	43
83	8:00	12:03	12	183	16:39	19:20	41	283	21:39	23:11	45
84	8:00	14:20	19	184	16:42	21:30	47	284	21:42	23:55	30
85	8:00	12:20	18	185	16:45	20:47	24	285	21:45	23:55	21
86	8:00	10:50	11	186	16:48	22:41	41	286	21:48	23:55	12
87	8:00	12:10	8	187	16:51	18:00	27	287	21:51	23:55	13
88	8:00	16:25	14	188	16:54	19:05	26	288	21:54	23:55	45
89	8:00	20:15	25	189	16:57	19:30	25	289	21:57	23:55	14
90	8:00	20:45	5	190	17:00	21:00	35	290	22:00	23:55	17
91	8:00	20:40	45	191	17:03	22:00	34	291	22:03	23:55	17
92	8:00	9:00	30	192	17:06	19:25	28	292	22:06	23:55	36
93	8:00	12:10	32	193	17:09	21:00	33	293	22:09	23:55	11
94	8:00	15:40	3	194	17:12	21:28	50	294	22:12	23:55	11
95	8:00	13:40	22	195	17:15	18:30	17	295	22:15	23:55	35
96	8:05	17:20	4	196	17:18	20:21	35	296	22:18	23:55	12
97	8:05	19:20	14	197	17:21	19:45	31	297	22:21	23:55	49
98	8:05	10:25	18	198	17:24	21:46	45	298	22:24	23:55	49
99	8:10	10:00	11	199	17:27	23:55	35	299	22:27	23:55	44
100	8:10	20:25	25	200	17:30	20:39	35	300	22:30	23:55	41
